Near Infra-Red Spectroscopy Predicts Crude Protein in Hemp Grain

Ryan Crawford[1], Jamie Crawford[1], Lawrence B. Smart[2], Virginia Moore[3]

[1]Cornell University, Ithaca, NY,
[2]Cornell AgriTech, Geneva, NY,
[3]Cornell University, Ithaca, NY,

Corresponding author: Ryan Crawford, rvc3@cornell.edu

Abstract

Lorem ipsum dolor sit amet, consectetur adipiscing elit, sed do eiusmod tempor incididunt ut labore et dolore magna aliqua. Ut enim ad minim veniam, quis nostrud exercitation ullamco laboris nisi ut aliquip ex ea commodo consequat. Duis aute irure dolor in reprehenderit in voluptate velit esse cillum dolore eu fugiat nulla pariatur. Excepteur sint occaecat cupidatat non proident, sunt in culpa qui officia deserunt mollit anim id est laborum.

Plain Language Summary

Earthquake data for the island of La Palma from the September 2021 eruption is found …

incomplete: may contain errors, run-ons, half-thoughts, etc.

0.1 INTRODUCTION

Hemp (Cannabis sativa L.) is an annual crop with potential uses as a source of food or feed from grain, and bast fiber or hurd from the stalk. Hemp cultivars are commonly grown for one or both purposes and a cultivar may be referred to as a grain, fiber, or dual-purpose type. Because of protein's nutritional importance, the protein content of a grain crop is an prime consideration for researchers, producers, and consumers. Whole hemp grain typically contains approximately 20-30% protein (Bárta et al., 2024; Callaway, 2004; Ely & Fike, 2022). Crude protein (CP) is often used as a proxy for the direct measurement of protein concentration and consists of the multiplication of nitrogen concentration by a conversion factor because measuring nitrogen concentration is relatively simple (Hayes, 2020).

Near-infrared spectroscopy (NIRS) technology is rapid, non-destructive, and cheap. It consists of the measurement of NIR radiation reflected and absorbed from a sample (the spectra) and the relation of the spectra to laboratory values for components such as moisture, protein, fat, or fiber (Roberts et al., 2004). NIRS technology has been used since the 1970's to assess forage CP (Reeves, 2012; Williams, 1975). A NIRS calibration set often consists of samples from one species grown in many environments encompassing the range of expected values from the analyte or analytes (Chadalavada et al., 2022). Partial least squares regression (PLSR) is a typical method used in the agricultural and food sciences to relate spectra to analyte (Roberts et al., 2004). PLSR calculates components that maximize covariance between predictor and response variables. PLSR uses some number of components, often selected via cross-validation, in order to fit the regression model and is commonly used in spectroscopy because it tends to work well with highly-correlated, noisy spectral data (Wold et al., 2001).

A NIRS-scanned sample of undamaged grain may used for other purposes besides its scan or it may planted as a seed. In wheat and corn, grain protein content has been shown to be heritable (Geyer et al., 2022; Giancaspro et al., 2019). This suggests (at least potentially) that NIRS technology could serve as resource to rapidly identify high CP hemp germplasm, enabling the screening of more germplam as grain, before planting to the field, and thus enabling the more efficient development of high CP hemp grain cultivars.

For this study, a benchtop NIR spectrometer was used to develop a model to predict CP content based on a data set of hemp grain representing multiple years, locations, and cultivars from grain and dual-purpose hemp types using PLSR.

0.2 MATERIALS AND METHODS

Source: Article Notebook

Source: Article Notebook

0.2.1 Hemp Grain Sample Background

Spectral data were obtained from whole (unground) hemp grain samples, harvested at maturity, collected from 2017 - 2021 from 18 cultivar trials in New York (NY) (NA samples). Grain samples were obtained by hand sampling or mechanical harvest and were cleaned of chaff and dried at 30 C for six days in a forced-air dryer. In total, 38 cultivars were represented in the data set. Cultivars were grain or dual-purpose types and included both commercially available and experimental material.

All cultivar trials were planted in randomized complete block design with each cultivar replicated four times. The 2017 data were comprised of samples from the same thirteen cultivars sampled from six NY locations. For those trials, grain was harvested from each plot individually and aggregated by cultivar within each trial. Four subsamples were drawn from each aggregated sample and scanned separately. These spectra were averaged at each 2 nm increment. All remaining samples from 2018-2021 were collected on a per-plot basis. All possible cultivars and possible locations were represented in 2017, but only a selected subset of cultivars and locations were represented in 2018-2021.

0.2.2 Spectral Data Collection and Preprocessing

A benchtop NIR spectrometer (FOSS/ NIR FOSS/ NIR Systems model 5000) was used to obtain the spectra (FOSS North America, Eden Prairie, MN, USA). Spectra were collected every 2 nm from 1100-2498 nm and the logarithm of reciprocal reflectance was recorded. A 1/4 rectangular sample cup (5.7 cm $\times$ 4.6 cm) was used.

WINISI software version 1.02A (Infrasoft International, Port Matilda, PA, USA) was used to average the spectra in 2017, as well as to select samples for laboratory assay. Samples were selected according to their spectral distance from their nearest neighbor within the calibration data set with a cutoff of a distance of 0.6 H, where H is approximately equal to the squared Mahalanobis distance divided by the number of principal components used in the calculation (Garrido-Varo et al., 2019). Prior to selection selection, spectra were preprocessed using SNV-detrend with settings 1,4,4,1 for the derivative, gap, smooth, and smooth 2 settings respectively.

0.2.3 Laboratory Validation

Laboratory assays were performed by Dairy One Forage Laboratory (Ithaca, NY). For those assays, 1mm ground samples were analyzed by combustion using a CN628 or CN928 Carbon/Nitrogen Determinator. Samples from 2017 were aggregated as described above, but the remaining samples were not aggregated.

0.2.4 Model Development

Calibration and validations sets were created by dividing the laboratory CP values into tertiles according to their percent CP in order to ensure that the range of CP values was present in both calibration and testing sets. Within each tertile, 75% of the samples were randomly assigned to the calibration set and the remaining 25% were assigned to the testing set. For each calibration set, models were developed in the caret package using PLSR. In fitting the model, the number of components was optimized over a grid search from 1-20. Model performance was evaluated with 25 iterations of bootstrapping and minimized root mean squared error (RMSE) in selecting the number of components in the final model .

Source: Article Notebook

Initially a number of common spectral preprocessing methods were tested by creating 100 calibration and testing sets, as described above. Spectral data from those data sets were transformed by each of the following methods: 1) first derivative, 2) Savitzky-Golay (SG) using the first derivative, third order polynomial, and a window of size 5, 3) gap-segment derivative using the first derivative, a gap of eleven, and a segment size of 5, 4) standard normal variate (SNV), 5) standard normal variate fol-

lowing Savitzky-Golay (SNV-SG) (same SG parameters as above), 6) SNV-detrend with second order polynomial, and 7) multiplicative scatter correction. As a comparison, models were also developed using untransformed spectra.

For each of these preprocessing methods, models were fit and predictions were made on the corresponding validation set (since there were 8 preprocessing methods, 8 separate models were fit for each of the 100 sets. The relationship between the predicted and actual values of the testing set were calculated via RMSE, R^2 and Ratio of Performance to InterQuartile distance (RPIQ), three common model assessment metrics. Larger R^2 and RPIQ, and smaller RMSE values are superior. Analyses of variance (ANOVA) were performed for each of these metrics in order to compare the preprocessing methods. For each ANOVA, each data set was considered as a subject and different variances were allowed for each preprocessing method.

Once the most promising preprocessing method was identified, 1000 more data sets were created and analyzed via that method and performance on the testing sets was summarized with RMSE, R^2, and RPIQ.

0.2.5 Additional software used

We used R version 4.3.3 (R Core Team, 2024) and the following R packages: caret v. 6.0.94 (Kuhn & Max, 2008), data.table v. 1.15.2 (Barrett et al., 2024), emmeans v. 1.10.0 (Lenth, 2024), nlme v. 3.1.163 (J. Pinheiro et al., 2023; J. C. Pinheiro & Bates, 2000), pls v. 2.8.3 (Liland et al., 2023), prospectr v. 0.2.7 (Stevens & Ramirez-Lopez, 2024), skimr v. 2.1.5 (Waring et al., 2022), tidymodels v. 1.1.1 (Kuhn & Wickham, 2020), tidyverse v. 2.0.0 (Wickham et al., 2019).

Source: Article Notebook

0.3 RESULTS AND DISCUSSION

0.3.1 Laboratory assay CP values

Laboratory assay percent CP values are summarized in the following table. These are similar to the range of CP values observed in the literature, indicating an reasonable basis for a chemometric model. The CP values are left-skewed and two thirds of the samples contained more than 25% CP.

Table 1: Summary of Laboratory Assayed CP Values (Percent Dry Matter)

Mean	Sd	Minimum	First Quartile	Median	Third Quartile	Maximum
26.1	2.5	20.8	23.9	26.4	28.2	30.8

Source: Article Notebook

0.3.2 Preprocessing methods comparison

Source: Article Notebook

Source: Article Notebook

Source: Article Notebook

Source: Article Notebook

Source: Article Notebook

Source: Article Notebook

All preprocessing methods outperformed untransformed spectral data Table 2. Averaged together, all preprocessed spectra were superior to untransformed spectra, with

lower RMSE, and higher R^2 and RPIQ values (significant at α level <0.001). Preprocessing methods had -11.6 % lower RMSE, and had 3.1% higher R^2 7.4% higher RPIQ than unprocessed spectra.

The SNV-SG method had the lowest RMSE, highest R^2, and highest RPIQ averaging over all iterations. SNV-SG RMSE averaged 1.4% lower, while R^2 and RPIQ averaged 0.4% and 2.4% higher respectively than the next best preprocessing method (SG in both cases), but the difference between the best and second best method by metric were only statistically significant at α <0.05 for RPIQ. RPIQ was devised to accurately reflect the spread of data in skewed populations (Bellon-Maurel et al., 2010) and thus offers a robust metric for model assessment in this context, where the CP data are skewed. Therefore the superiority of SNV-SG as measured via RPIQ made it the best choice for the final model.

Table 2: Evaluation of Preprocessing Methods by Metric ± Standard Error

Preprocessing Method	RMSE	R^2	RPIQ
Standard Normal Variate following Savitzky-Golay	1.02 ± 0.012	0.84 ± 0.004	3.97 ± 0.076
Savitzky-Golay	1.03 ± 0.012	0.83 ± 0.004	3.88 ± 0.072
First Derivative	1.07 ± 0.013	0.82 ± 0.004	3.77 ± 0.075
Standard Normal Variate	1.12 ± 0.016	0.80 ± 0.005	3.61 ± 0.081
Gap-segment Derivative	1.12 ± 0.018	0.81 ± 0.006	3.60 ± 0.086
Standard Normal Variate-Detrend	1.13 ± 0.015	0.80 ± 0.005	3.55 ± 0.079
Multiplicative Scatter Correction	1.17 ± 0.016	0.79 ± 0.006	3.47 ± 0.080
Untransformed Spectra	1.22 ± 0.044	0.79 ± 0.009	3.42 ± 0.105

Source: Article Notebook

These results are not surprising. SNV and SNV-detrend both correct light scatter, which is often a function of differences in particle size and sample packing density, although SNV-detrend is often used for densely-packed, powdered samples (Barnes et al., 1989). Here, hemp grain was neither powdered nor densely packed SG is a smoothing filter that regresses on the signal over a series of windows, removing noise while preserving the signal's shape and features.(Li et al., 2020; Luo et al., 2005). Derivatives remove noise, but not necessarily light scatte

cite: Barnes RJ, Dhanoa MS, Lister SJ. 1989. Standard normal variate transformation and de-trending of near-infrared diffuse reflectance spectra. Applied spectroscopy, 43(5): 772-777.

The preprocessing methods examined represent a portion of those available. As well, preprocessing methods tend to have a number of user-adjustable parameters whose various permutations were not tested. This subset of preprocessing methods and parameters nonetheless contained substantial variations in model quality, demonstrating the importance of the selection of an appropriate preprocessing method.

0.3.3 Final model development and summary

Source: Article Notebook

The model improved most rapidly as the number of principal components increased from 1 to 7, with the inclusion of each additional PC being associated with a decrease in RMSE of 5-12% . From 8 to 12 PCs, model performance continued to improve, although gains were more modest (decrease in RMSE of 0.7-3%). With 13 or more PCs, performance gains were minimal and the relative ranks of the models tended to be stable Figure 1.

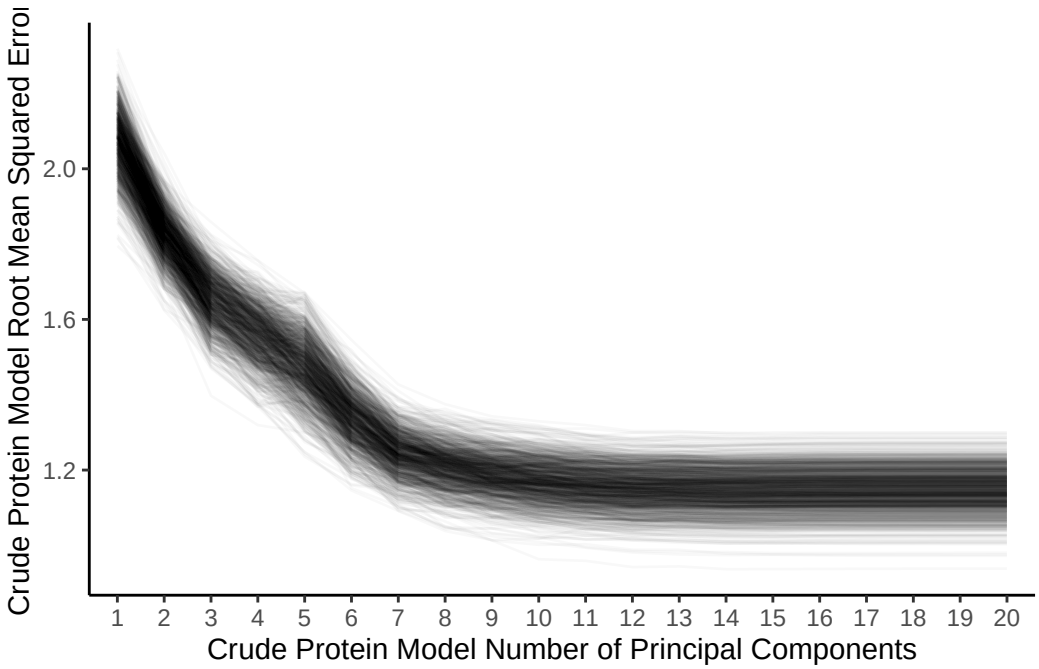

Figure 1: Decreasing RMSE with increasing number of PCs

Source: Article Notebook

Source: Article Notebook

Final model performance was similar, but not identical to, that obtained during the initial comparison of preprocessing methods. The final models' mean RMSE was 1.03, R^2 was 0.83, and RPIQ was 3.89 (all calculated on the test sets). Despite the generally good model performance, a subset of poor models can be seen. For example, Figure 2 shows twenty-one models with R^2 below 0.7. **more comment on poor models?**

Source: Article Notebook

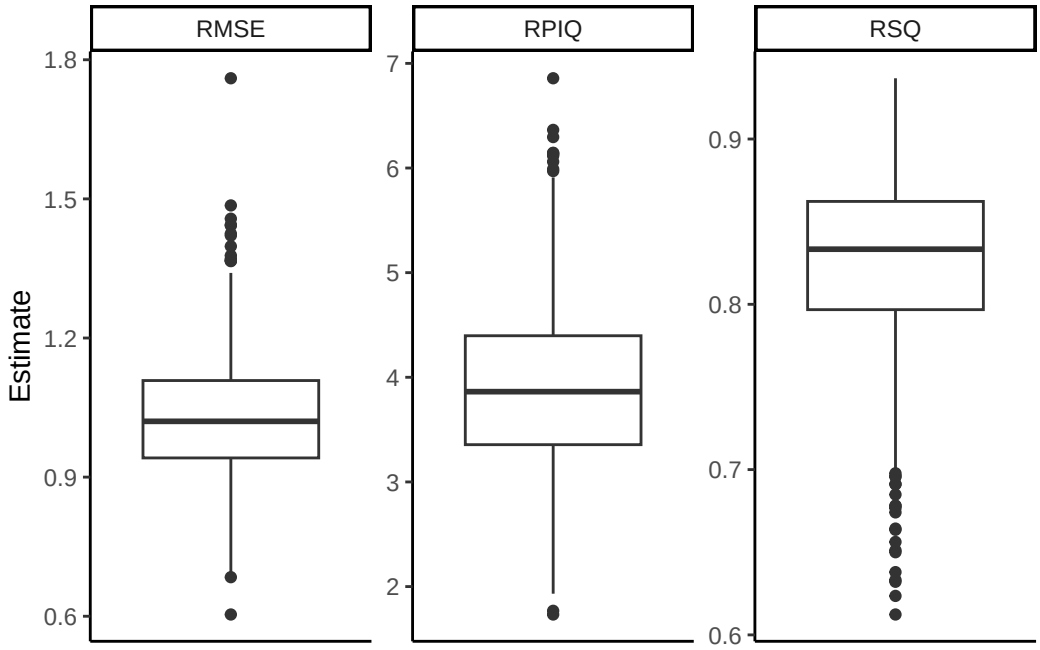

Figure 2: Final model validation set performance (1000 iterations)

Source: Article Notebook

Source: Article Notebook

Source: Article Notebook

```
Call:
lm(formula = difference ~ adj_cp, data = temp_dat)

Residuals:
     Min       1Q   Median       3Q      Max
-2.51794 -0.58132  0.06936  0.50754  2.74745

Coefficients:
            Estimate Std. Error t value Pr(>|t|)
(Intercept)  0.80412    0.17827   4.511 1.31e-05 ***
adj_cp      -0.15334    0.03051  -5.026 1.44e-06 ***
---
Signif. codes:  0 '***' 0.001 '**' 0.01 '*' 0.05 '.' 0.1 ' ' 1

Residual standard error: 0.9138 on 147 degrees of freedom
Multiple R-squared:  0.1466,    Adjusted R-squared:  0.1408
F-statistic: 25.26 on 1 and 147 DF,  p-value: 1.438e-06
```

Source: Article Notebook

Source: Article Notebook

Finally, the pattern of errors was examined on a per-sample basis. Figure 3

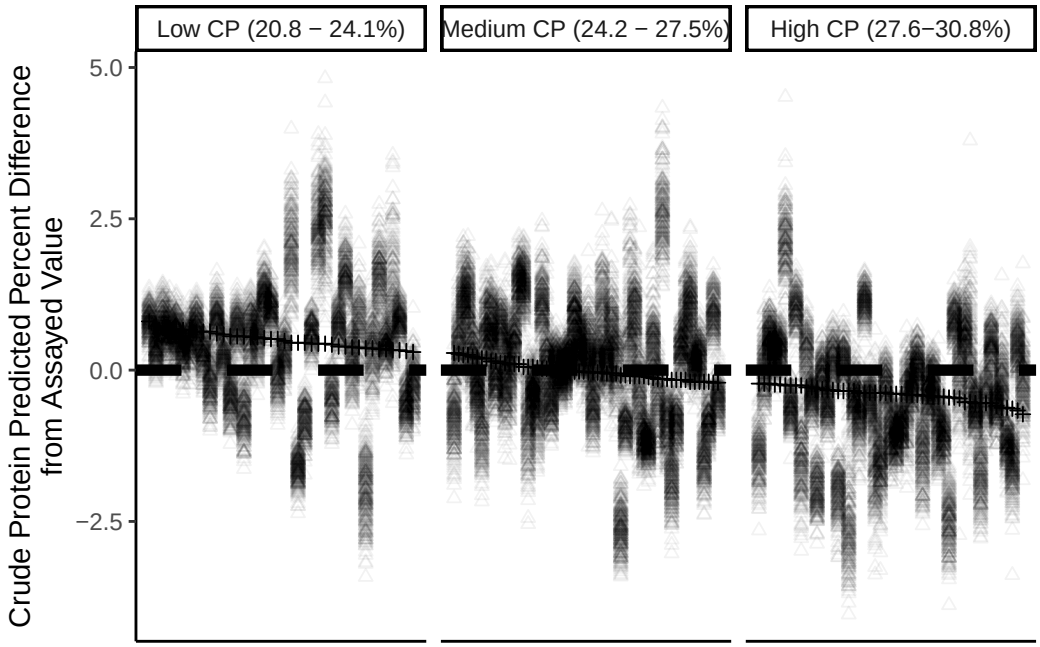

Figure 3: Test set prediction errors on a per-sample basis. Actual sample value set to 0, and samples ranked from least to greatest actual % CP value

Source: Article Notebook

Source: Article Notebook

To assess the patterns of errors within the models, a linear model was fit considering the mean estimated error for each sample considering all models where that sample was in the test set when compared to the sample's actual value. The models overestimated %CP by approximately 0.5 % in the lowest tertile and underestimated %CP by -0.01 % and -0.41 % in the middle and highest tertile, respectively

Key: <loc>

	loc	ith_in_data_set	crude_protein	difference	tmp_ith	adj_cp
	<char>	<int>	<num>	<num>	<int>	<num>
1:	cnoll	4	27.1	-1.826000348	90	6.3
2:	free	91	23.1	-1.608410140	24	2.3
3:	free	100	27.5	0.008386084	100	6.7
4:	free	103	26.0	-0.095290561	64	5.2
5:	freev	66	28.3	0.156805468	117	7.5
6:	freev	69	28.7	0.115415937	128	7.9
7:	freev	70	27.3	0.123941888	93	6.5
8:	ithaca	123	25.9	0.137420230	60	5.1
9:	ithaca	124	23.2	2.325322409	27	2.4
10:	ithaca	125	23.2	2.582685059	25	2.4
11:	ithaca	140	23.5	1.597167816	30	2.7
12:	ithaca	146	28.0	-1.965391942	110	7.2
13:	ithaca	148	26.4	0.145123025	76	5.6
14:	mcg	92	22.7	-0.110406545	20	1.9
15:	mcg	94	28.1	-0.067559276	111	7.3

```
    16:       mcg             121          28.3 -2.434565554     115    7.5
    17:      mg4e              28          25.4  0.034158139      53    4.6
    18:      mg4e              39          26.1 -0.016921027      66    5.3
    19:      mg4l              41          26.4  0.118021909      74    5.6
    20: rn041_gen             108          27.0  2.600884960      86    6.2
    21: rn041_gen             109          23.7 -1.980462540      33    2.9
    22: rn041_gen             110          29.0 -2.495337360     135    8.2
    23: rn041_gen             111          29.6 -1.777305991     140    8.8
    24: rn041_gen             113          29.5  0.011781362     139    8.7
    25: rn041_gen             114          27.7  2.115039075     107    6.9
    26:     rnooa              14          29.1 -0.003578789     137    8.3
    27:     rnooa              18          23.1  2.020690041      22    2.3
    28:     rnooa              19          25.3 -0.110141285      52    4.5
    29:     rnooa              25          26.6 -2.603177621      78    5.8
    30:     rnooa              26          28.3 -2.034162792     114    7.5
              loc ith_in_data_set crude_protein   difference tmp_ith adj_cp
                         grouping temp_id harv_year         cultivar         type
                           <char>   <int>     <int>           <char>       <char>
     1: worst_predicted_10_pct      32      2017            cfx-1
     2: worst_predicted_10_pct     111      2018           grandi        grain
     3:   best_predicted_10pct     128      2019            canda        grain
     4:   best_predicted_10pct     131      2019        nwg-elite         dual
     5:   best_predicted_10pct      94      2017           picolo
     6:   best_predicted_10pct      97      2017        futura 75
     7:   best_predicted_10pct      98      2017            cfx-1
     8:   best_predicted_10pct     155      2020         nwg-2730   multistate
     9: worst_predicted_10_pct     152      2020        futura 75 dual_replant
    10: worst_predicted_10_pct     156      2020    bialobrzeskie   multistate
    11: worst_predicted_10_pct       9      2021         logan c2         exp.
    12: worst_predicted_10_pct       5      2021            crs-1   grain_dual
    13:   best_predicted_10pct      10      2021  logan x anka c2         exp.
    14:   best_predicted_10pct     115      2018 nebraska (feral)         dual
    15:   best_predicted_10pct     113      2018           picolo        grain
    16: worst_predicted_10_pct     149      2019             h-51   multistate
    17:   best_predicted_10pct      56      2017            cfx-2
    18:   best_predicted_10pct      67      2017        futura 75
    19:   best_predicted_10pct      69      2017             anka
    20: worst_predicted_10_pct     136      2019        earlina 8        grain
    21: worst_predicted_10_pct     137      2019           katani        grain
    22: worst_predicted_10_pct     138      2019             joey        grain
    23: worst_predicted_10_pct     139      2019        futura 75         dual
    24:   best_predicted_10pct     141      2019             h-51         dual
    25: worst_predicted_10_pct     142      2019           hliana         dual
    26:   best_predicted_10pct      42      2017            tygra
    27: worst_predicted_10_pct      46      2017           katani
    28:   best_predicted_10pct      47      2017            cfx-2
    29: worst_predicted_10_pct      53      2017            cfx-1
    30: worst_predicted_10_pct      54      2017            wojko
                         grouping temp_id harv_year         cultivar         type
        in_ny      loc2
       <lgcl>    <char>
     1:   TRUE    geneva
     2:   TRUE freeville
     3:   TRUE freeville
     4:   TRUE freeville
```

```
 5:   TRUE freeville
 6:   TRUE freeville
 7:   TRUE freeville
 8:   TRUE    ithaca
 9:   TRUE    ithaca
10:   TRUE    ithaca
11:   TRUE    ithaca
12:   TRUE    ithaca
13:   TRUE    ithaca
14:   TRUE    ithaca
15:   TRUE    ithaca
16:   TRUE    ithaca
17:   TRUE    ithaca
18:   TRUE    ithaca
19:   TRUE    ithaca
20:   TRUE    geneva
21:   TRUE    geneva
22:   TRUE    geneva
23:   TRUE    geneva
24:   TRUE    geneva
25:   TRUE    geneva
26:   TRUE    geneva
27:   TRUE    geneva
28:   TRUE    geneva
29:   TRUE    geneva
30:   TRUE    geneva
     in_ny      loc2
```

Source: Article Notebook

This study is limited in that it represents the creation of one model based upon spectra collected from one machine. NIRS calibrations can be unique to a particular machine, even if the machines compared are of the same model (Reeves, 2012). As well, the calibration and validation sets are relatively small.

This research showed the promise of the use of NIRS in order to make predictions concerning %CP in hemp grain using PLS. Promising preprocessing methods were identified and a model was validated. Further research could refine a CP model by including more samples, identifying promising spectral regions, or by examining other predictive methods.

0.4 ACKNOWLEDGMENTS

0.5 SUPPLEMENTAL MATERIAL

Table 3: Tally of hemp cultivars and locations. Private cultivars are labeled "cultivar1", "cultivar2", etc.

cultivar2	chazy	freeville	geneva	ithaca	willsboro	Total
altair				1		1
anka		1	3	5	2	11
bialobrzeskie		1	3	4	1	9
canda		1	1	1		3
cfx-1		1	2	5		8
cfx-2		1	2	4		7
crs-1	1	1	2	5		9
cultivar1		1				1
cultivar2				1		1

Table 3: Tally of hemp cultivars and locations. Private cultivars are labeled “cultivar1”, “cultivar2”, etc.

cultivar2	chazy	freeville	geneva	ithaca	willsboro	Total
cultivar3				1		1
cultivar4				1		1
earlina 8			1			1
experimental1				1		1
experimental2				1		1
felina 32		1	2	3		6
futura 75		1	3	4		8
grandi		3	3	4		10
h-51			1	2		3
han-fn-h				1		1
han-nw				1		1
helena		1				1
henola				2		2
hlesia				3		3
hliana			1	1		2
joey		1	1	1		3
katani		2	3	4		9
nebraska (feral)	1			1		2
pewter river		1				1
picolo		1	2	5		8
portugal			1			1
rocky hemp			1			1
sterling gold			1			1
swift	1	1		1		3
tygra		1	3	4		8
uso-31	2	1	2	4		9
wojko		1	3	4		8
x-59		2		1		3
Total	5	24	41	76	3	149

Source: Article Notebook

0.6 OPTIONAL SECTIONS

0.7 REFERENCES

0.8 FIGURES AND TABLES

Source: Article Notebook

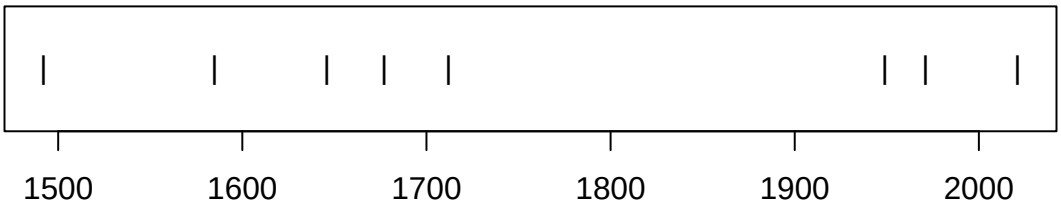

Figure 4: Timeline of recent earthquakes on La Palma

Source: Article Notebook

Source: Article Notebook

Based on data up to and including 1971, eruptions on La Palma happen every 79.8 years on average.

Studies of the magma systems feeding the volcano, such as (**marrero2019?**), have proposed that there are two main magma reservoirs feeding the Cumbre Vieja volcano; one in the mantle (30-40km depth) which charges and in turn feeds a shallower crustal reservoir (10-20km depth).

Eight eruptions have been recorded since the late 1400s (Figure 4).

Data and methods are discussed in Section 0.9.

Let x denote the number of eruptions in a year. Then, x can be modeled by a Poisson distribution

$$p(x) = \frac{e^{-\lambda}\lambda^x}{x!} \tag{1}$$

where λ is the rate of eruptions per year. Using Equation 1, the probability of an eruption in the next t years can be calculated.

Table 4: Recent historic eruptions on La Palma

Name	Year
Current	2021
Teneguía	1971
Nambroque	1949
El Charco	1712
Volcán San Antonio	1677
Volcán San Martin	1646
Tajuya near El Paso	1585
Montaña Quemada	1492

Table 4 summarises the eruptions recorded since the colonization of the islands by Europeans in the late 1400s.

La Palma is one of the west most islands in the Volcanic Archipelago of the Canary Islands (Figure 5).

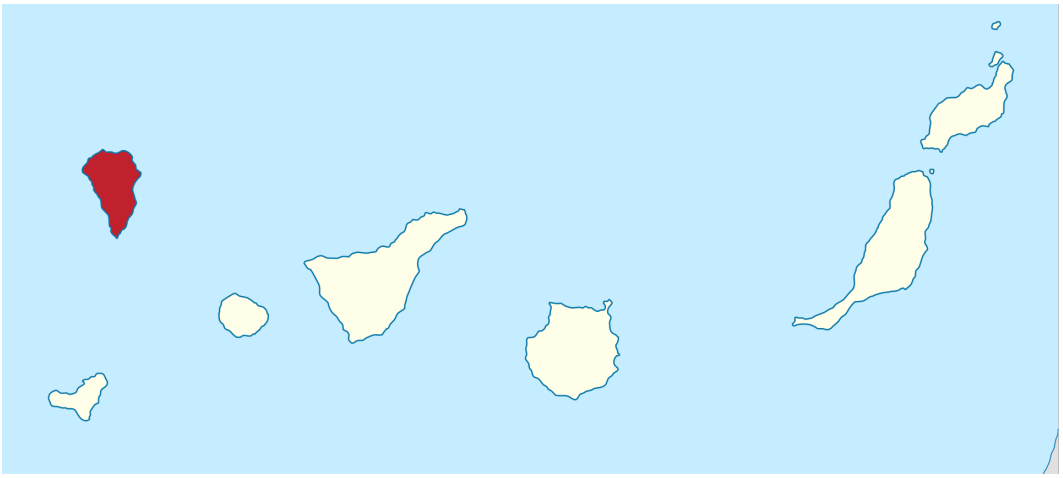

Figure 5: Map of La Palma

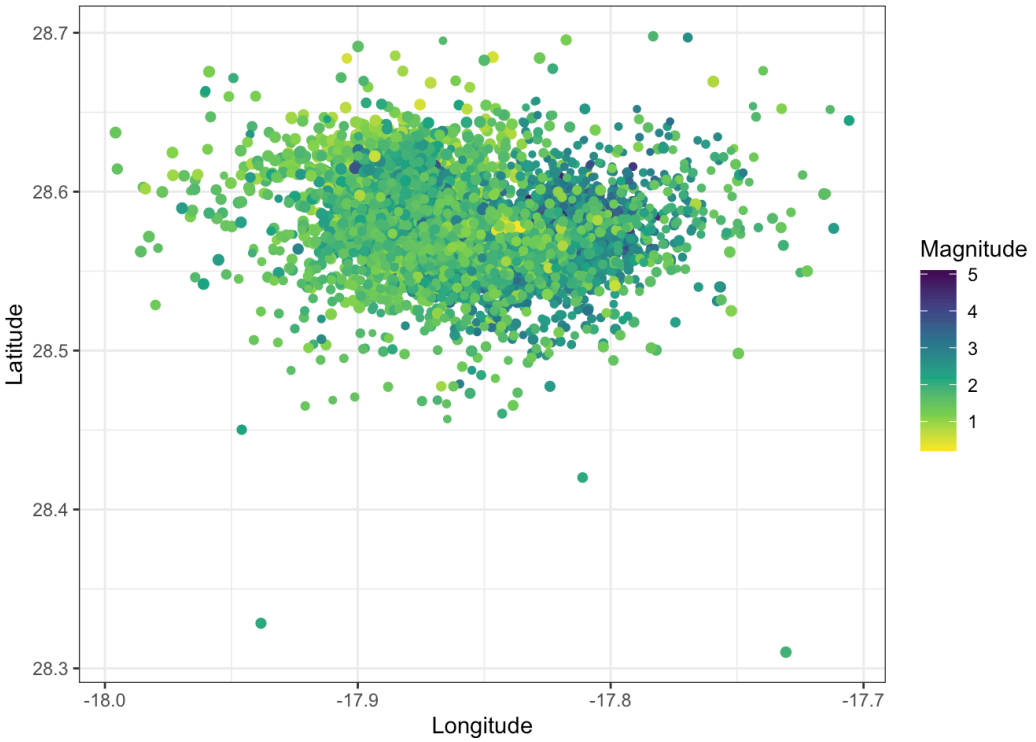

Figure 6: Locations of earthquakes on La Palma since 2017

Source: Explore Earthquakes

Figure 6 shows the location of recent Earthquakes on La Palma.

0.9 Data & Methods

0.10 Conclusion

References

Barnes, R. J., Dhanoa, M. S., & Lister, S. J. (1989). Standard Normal Variate Transformation and De-Trending of Near-Infrared Diffuse Reflectance Spectra. *Applied Spectroscopy*, *43*(5), 772–777. https://doi.org/10.1366/0003702894202201

Barrett, T., Dowle, M., Srinivasan, A., Gorecki, J., Chirico, M., & Hocking, T. (2024). *data.table: Extension of "data.frame"*. https://CRAN.R-project.org/package=data.table

Bárta, J., Roudnický, P., Jarošová, M., Zdráhal, Z., Stupková, A., Bártová, V., Krejčová, Z., Kyselka, J., Filip, V., Říha, V., Lorenc, F., Bedrníček, J., & Smetana, P. (2024). Proteomic Profiles of Whole Seeds, Hulls, and Dehulled Seeds of Two Industrial Hemp (Cannabis sativa L.) Cultivars. *Plants*, *13*(1), 111. https://doi.org/10.3390/plants13010111

Bellon-Maurel, V., Fernandez-Ahumada, E., Palagos, B., Roger, J.-M., & McBratney, A. (2010). Critical review of chemometric indicators commonly used for assessing the quality of the prediction of soil attributes by NIR spectroscopy. *TrAC Trends in Analytical Chemistry*, *29*(9), 1073–1081. https://doi.org/10.1016/j.trac.2010.05.006

Callaway, J. C. (2004). Hempseed as a nutritional resource: An overview. *Euphytica*, *140*(1), 65–72. https://doi.org/10.1007/s10681-004-4811-6

Chadalavada, K., Anbazhagan, K., Ndour, A., Choudhary, S., Palmer, W., Flynn, J. R., Mallayee, S., Pothu, S., Prasad, K. V. S. V., Varijakshapanikar, P., Jones, C. S., & Kholová, J. (2022). NIR Instruments and Prediction Methods for Rapid Access to Grain Protein Content in Multiple Cereals. *Sensors (Basel, Switzerland)*, *22*(10). https://doi.org/10.3390/s22103710

Ely, K., & Fike, J. (2022). Industrial Hemp and Hemp Byproducts as Sustainable Feedstuffs in Livestock Diets. In D. C. Agrawal, R. Kumar, & M. Dhanasekaran (Eds.), *Cannabis/Hemp for Sustainable Agriculture and Materials* (pp. 145–162). Springer. https://doi.org/10.1007/978-981-16-8778-5_6

Garrido-Varo, A., Garcia-Olmo, J., & Fearn, T. (2019). A note on Mahalanobis and related distance measures in WinISI and The Unscrambler. *Journal of Near Infrared Spectroscopy*, *27*(4), 253–258. https://doi.org/10.1177/0967033519848296

Geyer, M., Mohler, V., & Hartl, L. (2022). Genetics of the Inverse Relationship between Grain Yield and Grain Protein Content in Common Wheat. *Plants*, *11*(16), 2146. https://doi.org/10.3390/plants11162146

Giancaspro, A., Giove, S. L., Blanco, A., & Gadaleta, A. (2019). Genetic Variation for Protein Content and Yield-Related Traits in a Durum Population Derived From an Inter-Specific Cross Between Hexaploid and Tetraploid Wheat Cultivars. *Frontiers in Plant Science*, *10*. https://doi.org/10.3389/fpls.2019.01509

Hayes, M. (2020). Measuring Protein Content in Food: An Overview of Methods. *Foods*, *9*(10), 1340. https://doi.org/10.3390/foods9101340

Kuhn, M., & Wickham, H. (2020). *Tidymodels: A collection of packages for modeling and machine learning using tidyverse principles.* https://www.tidymodels.org

Kuhn, & Max. (2008). Building predictive models in r using the caret package. *Journal of Statistical Software*, *28*(5), 1–26. https://doi.org/10.18637/jss.v028.i05

Lenth, R. V. (2024). *emmeans: Estimated marginal means, aka least-squares means.* https://CRAN.R-project.org/package=emmeans

Li, Y., Huang, Y., Xia, J., Xiong, Y., & Min, S. (2020). Quantitative analysis of honey adulteration by spectrum analysis combined with several high-level data fusion strategies. *Vibrational Spectroscopy*, *108*, 103060. https://doi.org/10.1016/j.vibspec.2020.103060

Liland, K. H., Mevik, B.-H., & Wehrens, R. (2023). *pls: Partial least squares and principal component regression*. https://CRAN.R-project.org/package=pls

Luo, J., Ying, K., He, P., & Bai, J. (2005). Properties of Savitzky–Golay digital differentiators. *Digital Signal Processing*, *15*(2), 122–136. https://doi.org/10.1016/j.dsp.2004.09.008

Pinheiro, J. C., & Bates, D. M. (2000). *Mixed-effects models in s and s-PLUS*. Springer. https://doi.org/10.1007/b98882

Pinheiro, J., Bates, D., & R Core Team. (2023). *nlme: Linear and nonlinear mixed effects models*. https://CRAN.R-project.org/package=nlme

R Core Team. (2024). *R: A language and environment for statistical computing*. R Foundation for Statistical Computing. https://www.R-project.org/

Reeves, J. B. (2012). Potential of Near- and Mid-infrared Spectroscopy in Biofuel Production. *Communications in Soil Science and Plant Analysis*, *43*(1-2), 478–495. https://doi.org/10.1080/00103624.2012.641844

Roberts, C. A., Workman, J., & Reeves, J. B. (2004). *Near-infrared spectroscopy in agriculture*. American Society of Agronomy.

Stevens, A., & Ramirez-Lopez, L. (2024). *An introduction to the prospectr package*.

Waring, E., Quinn, M., McNamara, A., Arino de la Rubia, E., Zhu, H., & Ellis, S. (2022). *skimr: Compact and flexible summaries of data*. https://CRAN.R-project.org/package=skimr

Wickham, H., Averick, M., Bryan, J., Chang, W., McGowan, L. D., François, R., Grolemund, G., Hayes, A., Henry, L., Hester, J., Kuhn, M., Pedersen, T. L., Miller, E., Bache, S. M., Müller, K., Ooms, J., Robinson, D., Seidel, D. P., Spinu, V., … Yutani, H. (2019). Welcome to the tidyverse. *Journal of Open Source Software*, *4*(43), 1686. https://doi.org/10.21105/joss.01686

Williams, P. C. (1975). Application of near infrared reflectance spectroscopy to analysis of cereal grains and oilseeds. *Cereal Chemistry*, *52*(4 p.561-576), 576–561.

Wold, S., Sjöström, M., & Eriksson, L. (2001). PLS-regression: A basic tool of chemometrics. *Chemometrics and Intelligent Laboratory Systems*, *58*(2), 109–130. https://doi.org/10.1016/S0169-7439(01)00155-1